

Cite this article as: *****, et al. Effect of Temperature on the Interface Microstructure and Mechanical Properties of AZ31/Al/Ta Composites Pre-prepared by Vacuum Hot Compression Bonding [J]Rare Metal Materials and Engineering,

<https://doi.org/10.12442/j.issn.1002-185X.20240604>

Effect of Temperature on the Interface Microstructure and Mechanical Properties of AZ31/Al/Ta Composites Prepared by Vacuum Hot Compression Bonding

Yu Zhilei¹, Li Jingli¹, Han Xiuzhu², Li Bairui¹, Xue Zhiyong¹

¹ Institute for Advanced Materials, North China Electric Power University, Beijing 102208, China; ² Beijing Institute of Spacecraft System Engineering, Beijing 100094, China

Abstract: The Mg/Ta composite material exhibits both exceptional resistance to high-energy particle irradiation and lightweight characteristics, enabling it to more effectively address the requirements of future deep-space exploration. However, joining these two dissimilar metals is challenging due to their significant differences in properties. In this work, AZ31/Al/Ta composites were successfully prepared using the vacuum hot compression bonding (VHCB) method. The effect of hot compressing temperature on the interface microstructure evolution, phase constitution, and shear strength at the interface was investigated. Moreover, the interface bonding mechanisms of the AZ31/Al/Ta composites under the VHCB process conditions were explored. The results demonstrated that as the VHCB temperature increased, the phase composition of the interface between Mg and Al changed from the Mg-Al brittle IMCs ($Al_{12}Mg_{17}$, Al_3Mg_2) to the Al-Mg solid solution. Meanwhile, the width of the Al/Ta interface diffusion layer increased to 450°C compared to that at 400°C. The shear strengths were 24 MPa and 46 MPa at 400°C and 450°C, respectively. The interfacial bonding mechanism of AZ31/Al/Ta composites involves the coexistence of diffusion and mechanical meshing. Avoiding the formation of brittle phases at the interface can significantly improve interfacial bonding strength.

Key words: AZ31/Al/Ta composites; Microstructure; Mechanical properties; vacuum hot compression bonding

Deep space exploration is a significant indicator of a country's overall national strength and innovation capability. However, as exploration activities venture deeper into space, the materials used for deep-space exploration equipment encounter numerous challenges^[1,2]. The high-energy charged particles in the deep space environment pose a risk of causing radiation damage to electronic components in spacecraft, which could potentially impact exploration missions. Furthermore, the lightweight design is essential for advancing deep space exploration due to its influence on the carrying capacity of existing spacecraft. Therefore, there is an urgent need to develop a material that combines resistance to energetic particle irradiation with lightweight characteristics to meet the demands of future deep space exploration.

Currently, high atomic number (Z) metals such as Nb and Ta have excellent electron shielding effects and have been successfully used by NASA as high-energy electron shielding materials in the Juno Jupiter probe^[3-5]. Moreover, the analysis and calculation outcomes of the anti-radiation material system reveal that, for the same surface density, an optimized combination of low-Z materials (like Mg) and high-Z (Ta) materials can offer a superior shielding effect compared to a single high-Z material, along with effectively reducing the weight^[6-8]. However, due to the significant differences in physical and chemical properties (Ta melting point 2996°C, Mg melting point 650°C; Ta is a body-centered cubic (BCC) crystal structure, and Mg is a hexagonal close-packed (HCP) crystal structure) between Mg and Ta, effective diffusion or metallur-

Received date:

Foundation item: National Natural Science Foundation of China (No.52275308; No.52301146), The Fundamental Research Funds for the Central Universities (2023JG007), and funding from Shi Changxu Innovation Center for Advanced Materials (SCXKFJJ202207).

Corresponding author: Han Xiuzhu, Ph.D., Professor, Beijing Institute of Spacecraft System Engineering, Beijing 100094, P. R. China, Tel: 010-61771720, E-mail: xiuzhuan@163.com

Copyright © 2019, Northwest Institute for Nonferrous Metal Research. Published by Science Press. All rights reserved.

gical bonding cannot be formed. Therefore, it is relatively difficult to fabricate the Mg - Ta composite. Besides, there are few reports on the preparation of Mg - Ta composite materials both at domestic and international levels.

Due to the mutual solubility of aluminum (Al) with both magnesium (Mg) and tantalum (Ta), Al can act as a medium for joining the two metals, Mg and Ta, thereby facilitating the preparation of Mg/Ta metal composites. Meanwhile, the rolling method has been utilized to manufacture Mg/Al/Ta multi-layer composite plates^[9,10]. However, the process involves subjecting Mg, Al, and Ta sheets to differential heat treatment to achieve coordinated deformation during rolling. This includes the oxidation of the sheets and temperature control throughout the rolling process. Consequently, the rolling process requires high-quality equipment and environmental conditions, which leads to low production efficiency due to its complexity. Fortunately, vacuum hot compression bonding (VHCB) offers a new solution to address the aforementioned challenges. However, there are limited reports on the fabrication of Mg/Al/Ta layered composite sheets using the VHCB method. The VHCB is an innovative solid-state bonding technology that utilizes thermo-mechanical coupling to induce significant high-temperature plastic deformation in the interface region, thereby facilitating interface bonding and atomic diffusion, ultimately achieving metallurgical bonding of the interface^[11,12]. Meanwhile, VHCB exhibits outstanding bonding performance and higher bonding efficiency, making it particularly well suited for bonding dissimilar metals and alloys^[13-15]. Additionally, the Gleeble thermal simulator has the advantages of rapid heating speed, high heating temperature, and the capability of creating high-pressure and vacuum environments. Therefore, in this study, we investigated the optimal process for vacuum hot-compression bonding of Mg/Al/Ta dissimilar metal composites using a Gleeble thermal simulator.

The AZ31 magnesium alloy is extensively utilized because of its superior strength and ductility compared to pure magnesium. In this work, we aimed to prepare AZ31/Al/Ta dissimilar metal composites by the VHCB method. In addition, the feasibility of preparing AZ31/Al/Ta composite materials using the VHCB method under different temperature conditions, the microstructure of the interface, and the types and mechanical properties of the second phase formed during the VHCB process were analyzed. Furthermore, the interfacial bonding

mechanism of AZ31/Al/Ta composites was investigated. This will optimize the adaptability of the VHCB process and provide a fundamental theoretical basis for preparing AZ31/Al/Ta dissimilar metal composites.

1 Experiment

Herein, commercial AZ31 magnesium alloy sheets, Al foil, and pure Ta sheets were utilized as raw materials. The chemical compositions of these materials are provided in Tables 1, 2, and 3. The sample sizes are depicted in Fig.1 (AZ31: $\phi 16 \times 2$ mm, pure Ta: $\phi 16 \times 2$ mm, Al foil: $\phi 16 \times 0.1$ mm). Additionally, stainless steel was employed to fabricate and design the sleeve for assembling and fixing the experimental samples, as shown in Fig.1. Prior to the experiment, the materials were ground and smoothed using various types of SiC sandpaper. In particular, the surfaces of the Ta and Mg plates were polished with a copper wheel to enhance their surface roughness. Subsequently, they were immersed in an ethanol solution for ultrasonic cleaning to remove oil stains from their surfaces.

Table 1 The chemical compositions of AZ31 alloy(wt.%)

Element	Al	Si	Ca	Zn	Fe	Be	Mn	Cu	Mg
Content	3.19	0.02	0.04	0.81	0.005	0.10	0.33	0.05	Bal.

Table 2 The chemical compositions of Al foil (wt.%)

Element	Si	Zn	Fe	Mn	Cu	Mg	Ti	V	Al
Content	0.25	0.05	0.35	0.03	0.05	0.03	0.03	0.05	Bal.

Table 3 The chemical compositions of Ta Sheet (wt.%)

Element	C	H	O	Nb	Fe	W	Mo	Si	Ta
Content	0.01	0.015	0.015	0.05	0.005	0.01	0.01	0.005	Bal.

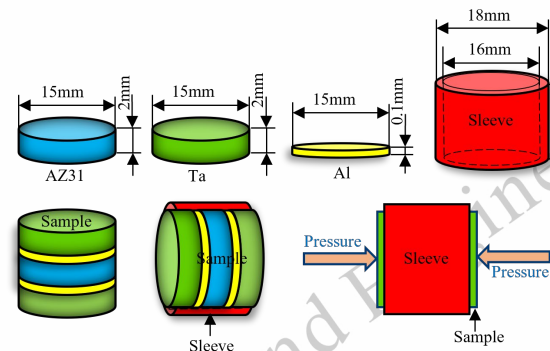


Fig.1 Sample size and assembly diagram

In the experiment, a Gleeble3800 Thermo-Mechanical Simulator (TMS) was used to conduct VHCB on the assembled samples. The schematic diagram of the Gleeble3800 VHCB process is depicted in Fig 2. (a). Initially, a k-type thermocouple (TC) with a diameter of 0.25 mm was spot welded onto the sample stainless-steel sleeve for temperature measurement

during the connection process. Subsequently, a small preload was applied to the specimen which was clamped between the TMS working pressure head. The thermocouple wire was then

Table 4 The vacuum hot compression bonding process

No.	Holding time (min)	Temperature (°C)	Pressure (MPa)	Bonding state
1	30	350	50	Al-Ta Unsuccessful
2	30	400	50	Successful
3	30	450	50	Successful

connected and the chamber was closed, followed by vacuuming the chamber to 1.33×10^{-4} mbar and initiating the hot compression cycle program. The process parameters are listed in Table 4. During the VHCB process, the sample was heated to the target temperature at a heating rate of 5°C/s . The sample was then loaded at a rate of 0.5MPa/s until it reached an experimental pressure of 50MPa , which was maintained for 30 min before concluding the VHCB process. Upon completion of the VHCB process, the applied load was rapidly released within one minute and subsequently cooled in the ambient air. The photos of vacuum hot-compression bonded samples are presented in Fig 2(b).

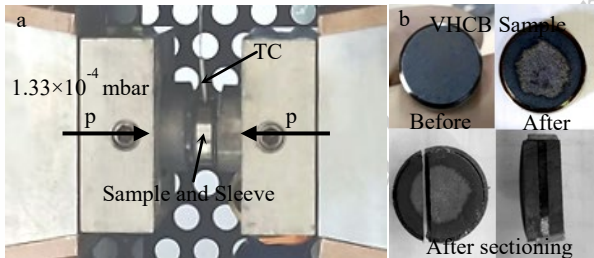


Fig. 2 (a) Schematic of the vacuum hot-compression bonding process using a Gleeble 3800, (b) Sample before and after vacuum hot-compression bonding.

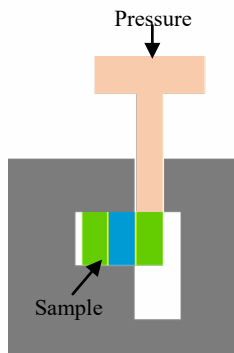


Fig.3 Schematic of the shear test measurement method.

The scanning electron microscope (SEM) observation and energy dispersive spectrometer (EDS) analysis were conduct-

ed using a Thermo Scientific Quattro field emission scanning electron microscope, equipped with an EDS system. The phase composition of the interface was determined by X-ray diffraction (XRD, Rigaku SmartLab SE). The XRD samples were obtained through the peeling method. Specifically, the Ta layer was removed, and XRD tests were performed on the Mg layer and exposed side of the intermediate layer. Fig.3 shows the schematic of the measuring method of the shear test. The shear test was performed using a universal testing machine at a loading rate of 0.2mm/min . At least three samples were tested for each process condition. The fracture surfaces were analyzed using SEM and EDS.

2 Results and Discussion

2.1 Influence of temperature on interlayer thickness

Fig.4 presents the interlayer thickness changes during the preparation of AZ31/Al/Ta layered composite materials using the VHCB technology under different temperature conditions. Fig. 4 (a) shows SEM images of the sample after undergoing the VHCB process at $50\text{MPa}/30\text{min}/350^\circ\text{C}$. It can be seen that under this process condition, the thickness of the Ta, Al, and AZ31 layers is 2mm , 0.1mm , and 2mm , respectively, which are the same as the initial ones before VHCB. When the VHCB process temperature increased to 400°C , the thickness of the Ta layer remained unchanged, while the thickness of the Al layer was no longer visible, and the thickness of the Mg layer was 1.6mm . Upon further increasing the temperature of the VHCB process to 450°C , as illustrated in Fig.4 (c), it was observed that the thickness of the Mg layer decreased further to 1.3mm .

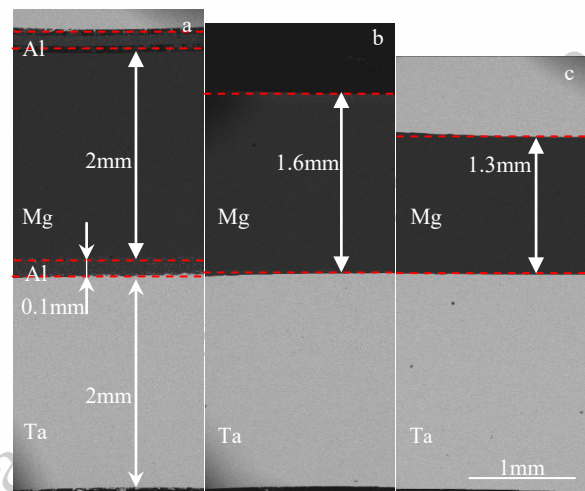


Fig.4 Interlayer thickness of VHCB samples: (a) 350°C , (b) 400°C , (c) 450°C .

During the experiments, it was found that the invisibility of the aluminum layer and the thinning of the magnesium layer were primarily caused by the spillage of molten magnesium-aluminum metal liquid during the VHCB process. It is worth noting that the VHCB process temperatures mentioned above did not reach the melting points of magnesium and aluminum, yet a phenomenon of melting still occurred. This was closely related to the heating principle of the Gleeble device. The Gleeble3800 TMS thermal control system operates by passing a low-frequency current through the sample, causing it to generate heat due to electric resistance^[15]. In the early stage of VHCB, the specimen was clamped with a small pre-load force, the Mg, Al, and Ta layer materials failed to adhere tightly between the surfaces, and the surfaces touched each other in the form of points, thereby forming a large contact electrical resistance at the contact interface. Therefore, the temperature in the point contact area is significantly higher during the heating process compared to other areas, which leads to the low melting point metals Mg and Al overheating and melting, forming a series of micro-region liquid phases between the interfaces. Simultaneously, owing to continuous and rapid heating, heat cannot be transferred in time. This leads to interface overheating triggered by microregion overheating, which further leads to more Mg and Al melting. After the short-term rapid heating was completed, quickly apply a target load of 50MPa. During the process of pressure loading, the molten Mg and Al liquid phases were squeezed and spilled out, resulting in a reduction in the interlayer thickness.

2.2 Interfacial structure and chemical compositions

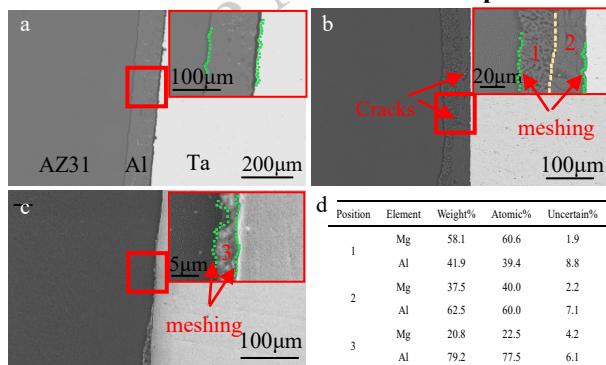


Fig.5 Scanning electron microscope (SEM) and energy dispersive spectrometer (EDS) results of the joints of samples:(a) 350°C, (b) 400°C, (c)450°C, (d) EDS results at positions 1, 2, and 3.

The microstructure photos at the interface of AZ31/Al/Ta samples after VHCB at different temperatures are shown in Fig.5. Fig.5 (a) shows the interface of the sample under the

conditions of 50MPa/30min/350 °C. It can be seen that the Mg/Al interface tightly contacts and binds under bonding pressure, with no formation of intermetallic compounds (IMCs) at the interface. The Al/Ta interface spalled during the cutting owing to its low bond strength. It can also be seen from Fig.5 (a) that a meshing shape is formed at the Al/Ta interface under pressure.

As depicted in Fig. 5 (b), effective bonding was successfully achieved at both Mg/Al and Al/Ta interfaces when the VHCB temperature reached 400 °C. Moreover, Fig.5 (b) shows that the interlayer thickness decreased to ~60µm. Simultaneously, a significant change in the morphology of the interlayer structure was observed, displaying distinct features on the side near Mg and Ta. Therefore, EDS analysis was conducted at interface positions 1 and 2, as shown in Fig.5(b). Fig.5(d) presents the chemical compositions at various locations. A layer with a thickness of 10~30µm can be formed close to the Mg side, which exhibits a stable stoichiometric proportion of Mg to Al (close to 17:12), indicating that this layer is composed of $Al_{12}Mg_{17}$ (γ)^[16-18]. Similarly, adjacent to layer 2, the content of Al and Mg is close to 3:2, suggesting that layer 2 is composed of Al_3Mg_2 (β)^[17-18]. Further observations showed that there were obvious microcracks in the formed IMCs. This was due to the plastic deformation of the composite material caused by the combined effect of pressure and temperature during the VHCB process. It is well known that IMCs have far higher hardness than matrix materials. Hence, plastic incompatibility during the VHCB process may result in cracks within the interlayer of hard and brittle IMCs^[19-20]. This also implies that the presence of such large brittle IMCs has a detrimental influence on the interfacial structure. Additionally, Fig. 5(b) illustrates that a meshing shape was formed at the interface, indicating that a mechanical meshing phenomenon also existed at the interface.

When the VHCB temperature was further increased to 450 °C, effective bonding was also achieved at the Mg/Al and Al/Ta interfaces, as shown in Fig.5(c). However, compared to the condition at 400°C, the thickness of the interlayer is significantly decreased. The EDS analysis was performed on interface region 3 (Fig. 5(c)). The results show that the contents of Mg and Al are 22% and 78% respectively, as shown in Fig. 5(d). This indicates that no brittle IMCs were formed under the process conditions of 450 °C. It is worth noting that the presence of a meshing shape at the interface was also ob-

served under this temperature condition.

The above results indicate that no Ta element was detected at the interface of the intermediate layer. This can be attributed to the high diffusion activation energy required for the migration of Ta atoms, which cannot be achieved under the aforementioned temperature conditions. Consequently, the Ta atoms did not diffuse to the interface.

Furthermore, it is noteworthy that a mechanical meshing phenomenon was observed at the interface in the aforementioned results, and previous studies have indicated that similar phenomena were also detected in rolling and explosive welding processes [21-23]. To enhance the mechanical properties of explosive-welded Al-Fe transition joints, Ming Yang et al. obtained the meshing interface by prefabricating dovetail grooves on the base plate [22-23]. Similarly, in order to enhance the interfacial bonding between Al and Ta, the surfaces of the Ta plate and Mg plate were roughened prior to thermal compression in this study. Therefore, during the vacuum hot compressing process, when the interfacial layer undergoes melting, the liquid metal phase will fill the irregular surfaces of Ta and Mg plates due to thermal-mechanical coupling effects, thereby forming a more microscopic mechanical meshing interface.

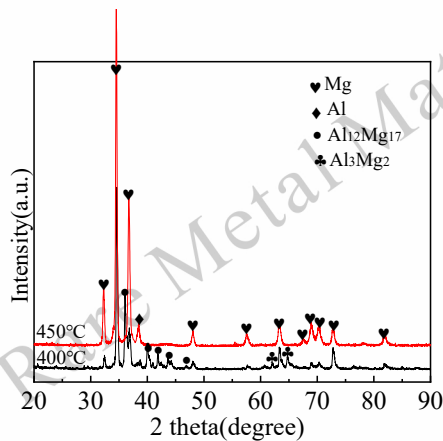


Fig.6 XRD results of the interfacial second phase of samples: 400°C and 450°C

The analysis of the SEM results above revealed that the second phase was only observed at the Mg/Al interface. To further clarify the phase composition of the interface during the VHCB process. The XRD analysis was performed on the Mg/Al interface of the samples (400°C and 450°C). The XRD results are presented in Fig.6. At 450°C, no second phase was detected at the Mg/Al interface, whereas at 400°C, the formation of Al_3Mg_2 and $\text{Al}_{12}\text{Mg}_{17}$ phases was evident. This further validates the accuracy of the above findings.

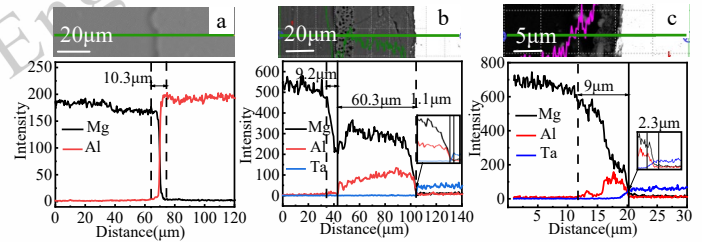


Fig.7 The line-scanning results in different samples: (a)350°C (b) 400°C (c)450°C

Fig.7 shows the line-scanning results under various temperature conditions. The elemental distribution of the Mg/Al bond interface line scanning results at 350 °C is shown in Fig.7(a). It can be observed that the Mg/Al interface diffusion layer thickness was $\sim 10.3\mu\text{m}$. As shown in Fig.7(b), when the temperature increases to 400°C, the thickness of the diffusion layer formed between Mg/Al, and Al/Ta is $\sim 69.5\mu\text{m}$ and $\sim 1.1\mu\text{m}$, respectively. Furthermore, when the VHCB temperature is increased to 450 °C, as illustrated in Fig. 7(c), it can be observed that the Mg/Al and Al/Ta interfaces are approximately $9\mu\text{m}$ and $2.3\mu\text{m}$, respectively.

The previously mentioned findings demonstrate that temperature significantly influences the interface structure and chemical composition. An appropriate temperature is an important parameter of the VHCB process [24,25]. Based on the above discussion, it can be concluded that as the temperature increases from 350 to 450°C, both the thicknesses of the diffusion layer and interface structure show significant differences. At 350°C, the bonding mechanism at the Mg/Al interface involved a combination of solid-state diffusion and mechanical meshing. The above findings also indicate weak mechanical meshing at the Al/Ta interface before peeling. When the temperature increased to 400°C and 450°C, both Mg/Al and Al/Ta interfacial bonding mechanisms were a combination of diffusion and mechanical meshing. Comparison of interface structures and chemical compositions of AZ31/Al/Ta composites fabricated using VHCB technology at 400°C and 450°C. A significant number of brittle intermetallic compounds ($\text{Al}_{12}\text{Mg}_{17}$ and Al_3Mg_2) were formed at the interface under the processing conditions of 400°C. In contrast, no brittle phases were observed at the interface under the processing conditions of 450°C. According to the Mg-Al binary phase diagram in the Mg-Al binary system, the liquid phase appears at a temperature of T_m ($T_m=437^\circ\text{C}$). Meanwhile, at the process temperature of 400°C, accompanied by the elimination of overheating, the supersaturated Mg-Al liquid phase at the interface

satisfied the thermodynamic conditions for the precipitation of Mg-Al IMCs during the cooling process to 400°C ($T < T_m$). Therefore, the IMCs are easily nucleated under these conditions. As the holding time increased, the IMCs gradually increased in size, eventually leading to the formation of large-sized γ and β IMCs. On the contrary, under the process conditions of 450°C, Mg-Al IMCs do not possess nucleation conditions during the process of interface cooling from overheated temperature to 450°C ($T > T_m$). The interface remains in the form of a eutectic liquid phase during this process, and in the subsequent long-term holding time process, the interface elements continue to diffuse and undergo isothermal solidification. Under this temperature process condition, the holding time stage after solidification also has the advantage of homogenization treatment, which can minimize element segregation and reduce the probability of generating Mg-Al IMCs to the maximum extent [26]. Furthermore, compared to 400°C, the width of the Al/Ta interface diffusion layer increased at 450°C. Overall, it can be assumed that the preparation of AZ31/Al/Ta composites by VHC technology at 450°C can yield an excellent interface structure.

2.3 Mechanical properties and fracture behavior of the interface

The room-temperature shear strengths of the samples under different temperature conditions are shown in Table 5. The shear strengths are 24 and 46 MPa at 400 °C and 450 °C, respectively. Compared with the process conditions at 400 °C, the shear strength of the AZ31/Al/Ta composite material was significantly improved at 450 °C.

Table 5 Shear strength of samples with different temperature conditions

Sample	Shear strength, (MPa)
50MPa×30min×350°C	---
50MPa×30min×400°C	24
50MPa×30min×450°C	46

The shear fracture surfaces on the Ta side microstructures of the samples at 400 °C and 450 °C are shown in Fig.8. The corresponding position elemental composition analysis of the fracture surface results is presented in Table 6. It shows the Ta matrix and Al_3Mg_2 phase, as indicated by the vertical arrows in Figs.8(a) and (b). This implies that the fracture of the bonded joints occurred mainly at the interface between the Al_3Mg_2 phase and Ta connection. Meanwhile, there is a large amount of parallel striation on the fracture surface, which can

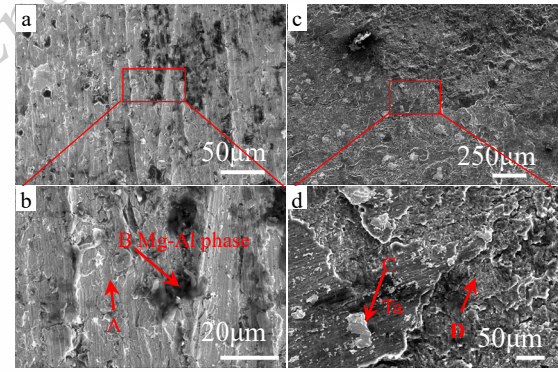


Fig.8 SEM images of fracture surfaces at Ta side of samples:

(a)(b)400°C (c)(d)450°C

be decided as brittle fracture characteristics [27]. The fracture of Mg-Al brittle IMCs may become the main cause of crack propagation and interface cracking [28]. The aforementioned results further suggest that the interfacial strength between the brittle phase and Ta was relatively weak. However, under the process conditions of 450 °C, as shown in Fig.8(c)(d). It shows that the fracture surface is mainly composed of a small amount of Ta and a large amount of Mg-Al alloy layer. This also implies that the fracture of the bonded joints occurred mainly on the interface between the Mg-Al alloy layer. This further indicates that the interfacial strength between the Mg-Al layer and Ta was relatively strong.

Table 6 Elemental composition analysis of the fracture surfaces (Fig. 8 a and b)

Position	Element	Weight%	Atomic%	Uncertain%
A	Mg	2.9	16.4	12.6
	Al	2.2	11.1	13
	Ta	95	72.5	7.3
B	Mg	38.4	40.9	2.4
	Al	61.6	59.1	6.7
C	Ta	100	100	7
	Mg	25.2	56.3	6.1
D	Al	12.4	24.9	8.7
	Ta	62.5	18.8	9.2

2.4 Summary of the technical principle of VHC technology for the preparation of AZ31/Al/Ta composites

Based on the above discussion and phase diagram analysis, the interface structure evolution model of the AZ31/Al/Ta composites prepared by VHC technology can be obtained, as shown in Fig.9. First, as shown in Fig.9 (a), in the early stage of the VHC, due to the unevenness of the material surface, there is a point contact phenomenon at the interface, which

leads to micro-zone overheating during the process of Gleeble

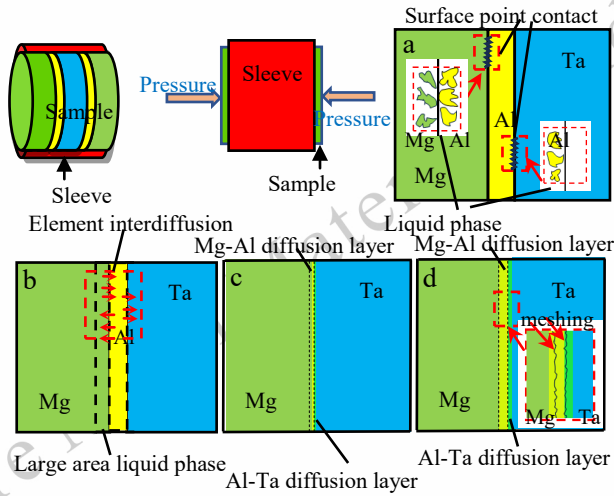


Fig.9 The Preparation technical principle of VHCb of AZ31/Al/Ta composites

heating to the target temperature ($T > T_m$). Therefore, several VHCb microregions are formed at the interface. Second, Fig.9 (b) shows that during the continuous heating process, micro-zone overheating triggers interface overheating, leading to the melting of Mg and Al and the formation of a large liquid-phase zone. Due to thermo-mechanical coupling, the Mg and Al liquid phases diffuse and fuse, while atomic diffusion occurs at the Al/Ta liquid-solid interface. As the pressure increased, the Mg and Al liquid phases filled the interface gaps, and the overheating phenomenon gradually subsided. During this period, the Al element continuously diffuses from the liquid phase into both sides of the base metal, further increasing the width of the liquid phase until the concentration of elements in the base metal and liquid phase reaches equilibrium in the phase diagram at the interface. Third, according to the equilibrium solidification lever law of the binary alloy phase diagram, as the alloy elements and base metal elements in the liquid phase diffuse into each other, the volume of the liquid phase gradually decreases, and isothermal solidification occurs during this process, as shown in Fig.9 (c). Accompanied by the process of solidification, a meshing shape begins to form at the interface under thermal-mechanical coupling. Finally, as shown in Fig.9 (d), there was still an uneven distribution of alloying elements after isothermal solidification. During the subsequent "keep warm" stage, the alloying elements undergo solid-phase diffusion, which leads to an increase in the width of the diffusion layer. This process further reduces element segregation and ultimately achieves a uniform inter-

facial element concentration.

Thus, from the above discussion, the AZ31/Al/Ta composites with good interfacial bonding properties can be obtained at a VHCb temperature of 450°C ($T > T_m$). Under this process condition, the AZ31/Al/Ta interface has uniform organization without forming a brittle second phase, creating a bonding interface where diffusion and mechanical meshing coexist.

3 Conclusions

In summary, the influence of temperature on the fabrication of AZ31/Al/Ta composite materials by using the VHCb method has been studied. The main conclusions of the present study are as follows:

- (1) The AZ31/Al/Ta composites were successfully prepared using the VHCb method with process parameters of $50\text{MPa}/30\text{min}/400^\circ\text{C}$ and $50\text{MPa}/30\text{min}/450^\circ\text{C}$.
- (2) The interfacial microstructure was significantly affected by temperature. Under the processing conditions of 400°C , a considerable amount of brittle intermetallic compounds ($\text{Al}_{12}\text{Mg}_{17}$, Al_3Mg_2) formed at the interface. In contrast, no brittle phases were formed at the interface under the processing conditions of 450°C .
- (3) The shear strengths were 24 MPa and 46 MPa at 400°C and 450°C , respectively. A VHCb temperature of 450°C exhibits a high shear strength because it avoids brittle phase formation at the interface.
- (4) The interface bonding mechanism of the AZ31/Al/Ta composite fabricated via the vacuum hot-pressing method was characterized by a synergistic combination of diffusion and mechanical meshing.

References

- [1] Sun Zezho, Meng Linzhi. *Journal of Nanjing University of Aeronautics & Astronautics* [J], 2015, 47(06):785-791. (in Chinese)
- [2] Pan Yongxin, Wang Chi. *Bulletin of National Natural Science Foundation of China* [J], 2021, 35(02):181-185. (in Chinese)
- [3] Zhao Kuo, Wen Chen, Sang Jie et al. *Space Electronic Technology* [J], 2021, 18(03):105-111. (in Chinese)
- [4] Lasi D, Tulej M, Meyer S, et al. *IEEE Transactions on Nuclear Science* [J], 2017, 64(1):605-613.
- [5] Fieseler P D, Ardalan S M., Frederickson A R. *IEEE Transactions on Nuclear Science* [J], 2002, 49(06):2739-2758.
- [6] Sicard-Piet A, Bourdarie S, Krupp N. *IEEE Transactions on Nuclear Science*. [J], 2011, 8(03), 923-931.

- [7] Chen Tuo, Tang Xiaobin, Chen Feida, *et al. Journal of Radiological Protection*[J], 2017, 37(02), 390–401.
- [8] Wang Jianzhao, Ma Jinan, Zhang Qingxiang, *et al. Spacecraft Environment Engineering*[J], 2019, 36(06):601-606. (in Chinese)
- [9] Han Xiuzhu, Luo Wenbo, Xue Zhiyong, *et al. CN202110658436.X*[P], 2021-09-07(in Chinese)
- [10] Yin Ziqing, Han Xiuzhu, Li Jingli, *et al. Journal of Netshape Forming Engineering*[J], 2023, 15(03):55-63. (in Chinese)
- [11] Sun Mingyue, Xu Bin, Xie Bijun, *et al. Journal of Materials Science & Technology*[J], 2021, 71(9):84-86.
- [12] Liao Yichuan, Lv Xuechao, Zhang Pengcheng, *et al. Rare Metal Materials and Engineering*[J], 2016, 45(7):1898~1902.
- [13] Zhou, Liying, Chen Wenxiong, Feng Shaobo, *et al. Journal of Materials Science & Technology*[J], 2020, 43:92-103.
- [14] Zhou Fangming, Zhang Fuqiang, Song Feiyuan, *et al. Rare Metal Materials and Engineering*[J], 2013, 42(9):1785~1789.
- [15] Li Chuanzong, Qian Xusheng, Zhang Maolong, *et al. Materials Characterization* [J], 2024, 211, 1044-5803.
- [16] Cui Xiaoming, Wang Zhengguang, Yu Zhilei, *et al. Rare Metal Materials and Engineering*[J], 2022, 51(04):1413-1419.
- [17] Liu Chuming, Zhu Xiurong, Zhou Haita, (*Phase Diagrams of Mg Alloy*), [M] Changsha: Central South University Press 2006. (in Chinese).
- [18] Chang Liang, Zheng Zhen tai, Cui Mengfei *et al. Materials Letters*[J], 2023, 331(15) 133495.
- [19] Qin Liang, Fan Minyu, Guo Xunzhong *et al. Vacuum* [J], 2018, 155: 96-107.
- [20] Liu Tingting, Guo Chuande, Tan Shijun *et al. Journal of Materials Engineering and Performance*[J], 2023, 31.
- [21] Liu Tingting, Song Bo, Huang Guangsheng, *et al. Journal of Magnesium and Alloys*[J], 2022, 10(8): 2062-2093.
- [22] Yang Ming, Ma Honghao, Shen Zhaowu, *et al. Transactions of Nonferrous Metals Society of China*[J], 2019, 29(4): 608-619.
- [23] Yang Ming, Ma Honghao, Shen Zhaowu, *et al. Fusion Engineering and Design* [J], 2019, 143:106-114.
- [24] M. Pouranvari, A. Ekrami, A. Kokabi. *Journal of Alloys & Compounds*[J], 2009, 469(1-2):270-275.
- [25] Li Mulan, Zhang Liang, Gao Lili, *et al. Intermetallics*[J], 2022:148.
- [26] X. Wang, (*Transient liquid-phase diffusion welding technology for metals*) [M] Beijing: Chemical Industry Press, 2021. (in Chinese)
- [27] Xiao Yi, Lang Lihui, Xu Wencai, *et al. Journal of Materials Research and Technology*[J], 2022, 19:1789-1797.
- [28] Liu Wensheng, Long Luping, Ma Yunzhu, *et al. Journal of Alloys and Compounds*[J], 2015, 643:34-39.

温度对真空热压连接技术制备 AZ31/Al/Ta 复合材料界面组织和力学性能的影响

于智磊¹, 李景利¹, 韩修柱², 李佰锐¹, 薛志勇¹

(1. 华北电力大学 先进材料研究院, 北京 102208)

(2. 北京空间飞行器总体设计部, 北京 100094)

摘要: Mg/Ta 复合材料兼具抗高能粒子辐照和轻质特性, 这使其能够更好的满足未来深空探测需求。然而, 由于这两种不同金属在性能上存在显著差异, 将它们连接起来颇具挑战性。本文采用真空热压连接方法成功制备了 AZ31/Al/Ta 复合材料。研究了热压温度对 AZ31/Al/Ta 复合材料界面组织演变、相组成及界面剪切强度的影响。探讨了 AZ31/Al/Ta 复合材料在 VHCB 工艺条件下的界面结合机理。结果表明, 随着热压温度的升高, Mg-Al 界面相组成由 Mg-Al 脆性 IMC ($Al_{12}Mg_{17}$, Al_3Mg_2) 转变为 Al-Mg 固溶体。与 400℃ 相比, 450℃ 时 Al/Ta 界面扩散层宽度增大。在 400℃ 和 450℃ 时, AZ31/Al/Ta 复合材料抗剪强度分别为 24 MPa 和 46 MPa。AZ31/Al/Ta 复合材料界面结合机制为扩散与机械啮合共存。此外, 避免界面脆性相的形成可以显著提高界面结合强度。

关键词: AZ31/Al/Ta 复合材料; 微观组织; 力学性能; 真空热压连接

作者简介: 于智磊, 男, 1994 年生, 博士生, 华北电力大学先进材料研究, 北京 102208, 电话: 010-61771720, E-mail: Zhileiyu_mail@ncepu.edu.cn